A general multipurpose interpolation procedure: The magic points

Article *in* Communications on Pure and Applied Analysis · October 2008

DOI: 10.3934/cpaa.2009.8.383 · Source: OAI

Yvon Maday
Sorbonne Université

Ngoc Cuong Nguyen
Massachusetts Institute of Technology

George Shu Heng Pau
Lawrence Berkeley National Laboratory

A general, multipurpose interpolation procedure: the magic points.

Yvon Maday* , Ngoc Cuong Nguyen† Anthony T. Patera‡ and George S. H. Pau§

August 14, 2007

Abstract

Lagrangian interpolation is a classical way to approximate general functions by finite sums of well chosen, pre-definite, linearly independent generating functions; it is much simpler to implement than determining the best fits with respect to some Banach (or even Hilbert) norms. In addition, only partial knowledge is required (here values on some set of points). The problem of defining the best sample of points is nevertheless rather complex and is in general not solved. In this paper we propose a way to derive such sets of points. We do not claim that the points resulting from the construction explained here are optimal in any sense. Nevertheless, the resulting interpolation method is proven to work under certain hypothesis, the process is very general and simple to implement, and compared to situations where the best behavior is known, it is relatively competitive.

1 Introduction

The extension of the reduced basis technique [8, 13, 15, 22, 24, 14] to nonlinear partial differential equations has led us to introduce an "*empirical Lagrangian interpolation*" method on a finite dimensional vectorial space spanned by functions that can actually be of any type (see [1, 7]). We refer to [19] for a general presentation to the reduced basis method. The efficiency of this approach in the reduced basis context, as outlined in [1, 7], and the simplicity of its implementation have stimulated us to deepen its analysis. The problem of Lagrangian interpolation is a classical one and, most of the times, it is associated with polynomial type approximations (algebraic polynomials, Fourier series, spherical harmonics, spline, rational functions, etc.). Given a finite dimensional space X_M in a Banach space X of continuous functions defined over a domain $\overline{\Omega}$ part of $\mathbb{R}$, $\mathbb{R}^d$ or $\mathbb{C}^d$, and a set of M points in $\overline{\Omega}$, $\{x_i \in \overline{\Omega}, i = 1, \ldots, M\}$, the interpolant of a function f in X is the (preferably unique) element f_M in X_M such that $f_M(x_i) = f(x_i), i = 1, \ldots, M$.

Among the classical questions raised by the interpolation process are

1. given a set of points, does the interpolant at these points exist;
2. is this interpolant unique;
3. how does the interpolation process compare with other approximations (in particular orthogonal projections);
4. is there an optimal selection for the interpolation points; and
5. is there a constructive optimal selection for the interpolation points.

*Université Pierre et Marie Curie-Paris6, UMR 7598, Laboratoire J.-L. Lions, Paris, F-75005 France and Division of Applied Mathematics, Brown University 182 George Street, Providence, RI 02912, USA, Email : maday@ann.jussieu.fr

†Department of Aeronautics & Astronautics, Massachusetts Institute of Technology, Cambridge MA02139, USA.

‡Department of Mechanical Engineering, Massachusetts Institute of Technology, Cambridge MA02139, USA.

§Department of Mechanical Engineering, Massachusetts Institute of Technology, Cambridge MA02139, USA.

The theory for *polynomial* interpolation is the best documented; however, even though it is rather complete nowadays in one dimension and partially over domains of simple shapes in higher dimensions (e.g. those obtained through tensor-product operations), the answers to these questions are rather complex and recent relative to the classical character of the questions.

Our interest is motivated by the broad framework where we have a set $\mathcal{U} \subset X$ that is supposed to be approximable by finite expansions involving given generating functions. In order to make this statement accurate, we can for instance consider that $\mathcal{U}$ has small *n-width* in the sense given by Kolmogorov [11, 20]. Let us remind that the *Kolmogorov n-width* of $\mathcal{U}$ in X is defined by

$$d_n(\mathcal{U}, X) = \inf_{X_n} \sup_{x \in \mathcal{U}} \inf_{y \in X_n} \|x - y\|_X \tag{1}$$

where X_n is some (unknown) n-dimensional subspace of X. The n-width of $\mathcal{U}$ thus measures the extent to which $\mathcal{U}$ may be approximated by some finite dimensional space of dimension n. There are many reasons why this n-width may go rapidly to zero as n goes to infinity. If $\mathcal{U}$ is a set of functions defined over a domain Ω, we can refer to regularity, or even to analyticity, of these functions with respect to the variable. Indeed, an upper bound for the asymptotic rate at which it converges to zero is provided by the example in [11] — $d_n(\tilde{B}_2^{(r)}; L^2) = \mathcal{O}(n^{-r})$ where $\tilde{B}_2^{(r)}$ is the unit ball in the Sobolev space of all 2π-periodic real valued, $(r-1)$-times differentiable functions whose first $(r-1)$ derivative is absolutely continuous and whose rth derivative belongs to L^2. Furthermore, exponential small n-width is achieved when analyticity exists in the parameter dependency.

Another possibility, that we actually encounter in the reduced basis framework is given by $\mathcal{U} = \{u(\mu, \cdot), \mu \in \mathcal{D}\}$, where, $\mathcal{D}$ is a given (infinite) set of parameters (either in $\mathbb{R}^p$ or even in some functional space of continuous functions). Then, the regularity of u in μ can also be a reason for having a small n-width.

Assuming that X is provided with a scalar product, then the best fit of an element $u \in \mathcal{U}$ in some finite dimensional space X_M that realizes almost the infimum in (1) is given by the orthogonal projection onto X_M. In many cases the evaluation of this projection may be costly and the knowledge of u over the entire domain Ω is required. Thus, assuming that $X \subset \mathcal{C}^0(\overline{\Omega})$, so that the elements in $\mathcal{U}$ are continuous, the interpolation is a tool that is often referred to as a inexpensive surrogate to the evaluation of the orthogonal projection.

In one space dimension, the polynomial interpolation is rather well understood : the only condition for a Lagrangian interpolation operator to exist is that the points are distinct. The location of almost optimal points is provided by the Chebyshev Gauss nodes. In dimension greater than one, there exist more intricate conditions in order for a polynomial interpolation to be well defined, and not any set of points would provide a positive answer to questions (1) and (2). For general functions — as the one we have in mind for reduced basis approximations (the functions are solutions of parameter dependent partial differential equations or functional in [4, 7]) — the general conditions for which the interpolation points give an unique interpolant is an open problem. Our proposed method provides a constructive approach to this general problem and partially answer the 5 questions raised above. Actually, our algorithm provides also an answer to an additional question : what are the generating functions we should use for interpolation.

In section 2, we explain the construction of these interpolating functions and the associated points that we have named *"magic points"*. We introduce the notion of Lebesgue constant and state some results related to the analysis of this approximation. In section 3, we compare the quality of this new general approach to some standard results in classical algebraic polynomial approximations of some typical geometries; we further demonstrate the versatility of the method with a nonstandard geometry. In section 4, we examine non-polynomial spaces and spaces spanned by parameter-dependent functions. In Section 5, we propose two applications of this procedure to approximate solutions of some PDEs, including a brief description of its application within reduced-basis methods. Lastly, we demonstrate how the *a posteriori* error estimator can be exploited in the construction of the approximation space.

We wish to stress that the applicability of the procedure is not limited to examples we have included in this paper; on the contrary, the procedure may prove advantageous in a variety of applications, for example image or data compression involving domains of irregular profile, fast rendering and visualization in animation, the development of computer simulation surrogates or experimental response surface for design and optimization, and the determination of a good numerical integration scheme for smooth functions on irregular domains. Lastly, for another approach to approximating parameterized fields, in particular an optimization–based approach well-suited to noisy data or constrained systems, see [16].

2 Empirical interpolation

We begin by describing the construction of the empirical interpolation method — a generalization of the one sketched in [1] and presented in greater details in [7]. The present construction allows us to define simultaneously the set of generating functions and the associated interpolation points. It is based on a greedy selection procedure as outlined in [18, 22, 23]. In what follows, we assume that the functions in $\mathcal{U}$ are at least continuous over the domain $\overline{\Omega}$. With $\mathcal{M}$ being some given large number, we assume that the dimension of the vectorial space spanned by $\mathcal{U}$: span $(\mathcal{U})$ is of dimension $\geq \mathcal{M}$.

To begin, we choose our first generating function u_1 as being defined by $u_1 = \arg\max_{u\in\mathcal{U}} \|u(\,\cdot\,)\|_{L^\infty(\Omega)}$[1]. We then define the first interpolation point as being $x_1 = \arg\max_{x\in\overline{\Omega}} |u_1(x)|$ then set $q_1 = u_1(\cdot)/u_1(x_1)$ and $B^1_{11} = 1$. We now construct, by induction, the nested sets of interpolation points $T_M = \{x_1, \ldots, x_M\}, 1 \leq M \leq M_{\max}$, and the nested sets of basis functions $\{q_1, \ldots, q_M\}$, where $M_{\max} \leq \mathcal{M}$ is some given upper bound fixed *a priori*. For $M = 2, \ldots, M_{\max}$, we first solve the interpolation problem for $\alpha_{M-1,j}[u], 1 \leq j \leq M$, from (assuming that the invertibility of the $(M-1)\times(M-1)$ matrix of running entry $q_j(x_i)$)

$$\sum_{j=1}^{M-1} q_j(x_i)\alpha_{M-1,j}[u] = u(x_i), \quad i = 1, \ldots, M-1 \ , \tag{2}$$

and compute

$$\mathcal{I}_{M-1}[u(\cdot)] = \sum_{j=1}^{M-1} \alpha_{M-1,j}[u] q_j \ , \tag{3}$$

We then set

$$\varepsilon_{M-1}(u) = \|u - \mathcal{I}_{M-1}[u]\|_{L^\infty(\Omega)} \ , \tag{4}$$

for all $u \in \mathcal{U}$; we define

$$u_M = \arg\max_{u\in\mathcal{U}} \varepsilon_{M-1}(u) \ , \tag{5}$$

and

$$x_M = \arg\max_{x\in\overline{\Omega}} |u_M(x) - \mathcal{I}_{M-1}[u_M](x)| \ , \tag{6}$$

we finally set $r_M(x) = u_M(x) - \mathcal{I}_{M-1}[u_M(x)]$, $q_M = r_M/r_M(x_M)$ and $B^M_{ij} = q_j(x_i), 1 \leq i,j \leq M$. The Lagrangian functions are used to build the interpolation operator $\mathcal{I}_M$ in $X_M = \text{span}\,\{u_i, 1 \leq i \leq M\}$ $= \text{span}\,\{q_i, 1 \leq i \leq M\}$ over the set of points $T_M = \{x_i, 1 \leq i \leq M\}$: for any given M, $\mathcal{I}_M[u(\,\cdot\,)] = \sum_{i=1}^M u(x_i) h_i^M(\,\cdot\,)$, where $h_i^M(\,\cdot\,) = \sum_{j=1}^M q_j(\,\cdot\,)[B^M]^{-1}_{ji}$ (note indeed that $h_i^M(x_j) = \delta_{ij}$).

We now demonstrate that this construction of the interpolation points $\{x_i, 1 \leq i \leq M\}$ and the basis functions $\{q_i, 1 \leq i \leq M\}$ is well-defined, meaning that the set $\{q_i, 1 \leq i \leq M\}$ is linearly independent and, in particular, the matrix B^M is invertible. We first prove an intermediate result:

Lemma 1. *Assume that $X_{M-1} = \text{span}\,\{q_1, \ldots, q_{M-1}\}$ is of dimension $M-1$ and that B^{M-1} is invertible, then we have $\mathcal{I}_{M-1}[v] = v$ for any $v \in X_{M-1}$; here $\mathcal{I}_{M-1}[v]$ is the interpolant of v as given below*

$$\mathcal{I}_{M-1}[v] = \sum_{j=1}^{M-1} \beta_{M-1,j} q_j \ , \tag{7}$$

[1] In case $\mathcal{U}$ is e.g. invariant by multiplication by a scalar, the max in the above formula is $= +\infty$ of course we should then replace it by e.g. $u_1 = \arg\max_{u\in\mathcal{U}} \frac{\|u(\,\cdot\,)\|_{L^\infty(\Omega)}}{\|u(\,\cdot\,)\|_X}$

where the $\beta_{M-1,j}$ is the solution of

$$\sum_{j=1}^{M-1} q_j(x_i)\beta_{M-1,j} = v(x_i), \quad i = 1, \ldots, M-1 \ . \tag{8}$$

In other words, the interpolation is exact for all v in X_{M-1}.

Proof. For $v \in X_{M-1}$, which can be expressed as $v(x) = \sum_{j=1}^{M-1} \gamma_{M-1,j} q_j(x)$, we consider $x = x_i, 1 \leq i \leq M-1$, to arrive at $v(x_i) = \sum_{j=1}^{M-1} q_j(x_i)\gamma_{M-1,j}, 1 \leq i \leq M-1$. It thus follows from the invertibility of B^{M-1} that $\beta_{M-1} = \gamma_{M-1}$; and hence $\mathcal{I}_{M-1}[v] = v$. □

We use the above result to prove

Theorem 1. *Assume that $M_{\max}$ is chosen such that $M_{\max} < \mathcal{M}$; then, for any $M \leq M_{\max}$, the space $X_M = span\{q_1, \ldots, q_M\}$ is of dimension M. In addition, the matrix B^M is lower triangular with unity diagonal (hence it is invertible).*

Proof. We shall proceed by induction. Clearly, $X_1 = \text{span}\,\{q_1\}$ is of dimension 1 and the matrix $B^1 = 1$ is invertible. Next we assume that $X_{M-1} = \text{span}\,\{q_1, \ldots, q_{M-1}\}$ is of dimension $M-1$ and the matrix B^{M-1} is invertible; we must then prove (i) $X_M = \text{span}\{q_1, \ldots, q_M\}$ is of dimension M and (ii) the matrix B^M is invertible. To prove (i), we note from our "arg max" construction that $\varepsilon_{M-1}(u_M) \geq \varepsilon_0$, where ε_0 — the Kolmogorov $M_{\max}$-width of $\mathcal{U}$ — is strictly positive since $M_{\max} < \mathcal{M}$. Hence $\varepsilon_{M-1}(u_M) > 0$, now if $\dim(X_M) \neq M$, we have $u(\,\cdot\,, \mu_M) \in X_{M-1}$ and thus $\varepsilon_{M-1}(\mu_M) = 0$ by Lemma 1, which raises the contradiction and ends the proof that $\dim(X_M) = M$ and $r_M(x_M) \neq 0$. To prove (ii), we just note from the construction procedure that $B^{M-1}_{i\,j} = r_j(x_i)/r_j(x_j) = 0$ for $i < j$; that $B^M_{i\,j} = r_j(x_i)/r_j(x_j) = 1$ for $i = j$; and that $\left|B^M_{i\,j}\right| = |r_j(x_i)/r_j(x_j)| \leq 1$ for $i > j$ since $x_j = \arg\max_{x \in \overline{\Omega}} |r_j(x)|, 1 \leq j \leq M$. Hence, B^M is lower triangular with unity diagonal. □

The error analysis of the interpolation procedure classically involves the Lebesgue constant $\Lambda_M = \sup_{x\in\Omega} \sum_{i=1}^M |h_i^M(x)|$. It has been proven in [7] that an upper-bound for the Lebesgue constant is $2^M - 1$ (in practice it turns out to be a very pessimistic upper bound, see however appendix A where we prove that this upper bound can be achieved). We remind also that the Lebesgue constant enters into the bound for the interpolation error as follows

Lemma 2. *For any $u \in X$, the interpolation error satisfies*

$$\|u - \mathcal{I}_M[u]\|_{L^\infty(\Omega)} \leq (1 + \Lambda_M) \inf_{v_M \in \text{span}\,\{u_i(\cdot), 1 \leq i \leq M\}} \|u - v_M\|_{L^\infty(\Omega)}. \tag{9}$$

The last term in the right hand side of the above inequality is known as the best fit of u by elements in span $\{u_i, 1 \leq i \leq M\}$.

The following result, extends to the interpolation process the proof in [3] for the best approximation. It makes much more precise the previous lemma, since it allows to state that even though we do not know finite dimensional spaces — candidates for achieving the minimal distance in the n-width — the greedy process for the magic points provides spaces that give an upper bound for the right hand side in (9). Indeed, we can prove that

Theorem 2. *Assume that $\mathcal{U} \subset X \subset L^\infty(\Omega)$, and that there exists a sequence of finite dimensional spaces*

$$\mathcal{Z}_1 \subset \mathcal{Z}_2 \subset \cdots \subset \mathcal{Z}_M \subset \cdots \subset \text{span}\,\mathcal{U}, \quad \dim \mathcal{Z}_M = M \tag{10}$$

such that there exists $c > 0$ and $\alpha > \log(4)$ with

$$\forall u \in \mathcal{U}, \inf_{v_M \in \mathcal{Z}_\mathcal{M}} \|u - v_M\|_X \leq c e^{-\alpha M} \tag{11}$$

then,

$$\|u - \mathcal{I}_M[u]\|_{L^\infty(\Omega)} \leq c e^{-(\alpha - \log(4))M}. \tag{12}$$

Proof. Refer to Appendix B. □

Remark 1. *This theorem states that, under the reasonable condition that the reduced space allows an exponential convergence (actually even faster convergence is observed most of the times, as explained in [3]), the empirical interpolation procedure : (i) proposes a discrete space (spanned by the chosen u_i) where the best fit is good, (ii) provides a set of interpolation points that leads to a convergent interpolant.*

Remark 2. *If for some reasons, a set of functions $u_i \in \mathcal{U}$, $i \in \mathbb{N}$ were to be given, all linearly independent, then the procedure of finding the interpolation points through the process $\forall i, 1 \leq i \leq M-1, \quad u(x_i) = \sum_{j=1}^{M-1} \alpha_{i,j}[u]u_j(x_i)$ and set $x_M = \arg\max_{x\in\overline{\Omega}} |u_M(x) - \sum_{j=1}^{M-1} \alpha_{i,j}[u_M]u_j(x)|$ is also well defined and leads to a set of interpolation points that have similar properties as above. The rational for the greedy approach is that it allows us to get a better sense of the interpolation properties since $\forall u$,*

$$\|u(\,\cdot\,) - \mathcal{I}_M[u(.)]\|_{L^\infty(\Omega)} \leq \|u_{M+1}(\,\cdot\,) - \mathcal{I}_M[u_{M+1}(\,\cdot\,)]\|_{L^\infty(\Omega)} = \varepsilon_M(x_{M+1}) \tag{13}$$

and this last quantity is one of the outputs of the construction process.

Remark 3. *In the actual implementation of the method, since the cardinal of $\mathcal{U}$ is infinite, we start with a large enough sample subset W^u in $\mathcal{U}$ of cardinal $\mathcal{M}$ much larger than the dimension of the discrete spaces and number of interpolation nodes we plan to use. For example, if $\mathcal{U} = \{u(\mu, \cdot), \mu \in \mathcal{D}\}$, we choose $W^u = \{u(\mu), \mu \in \Xi_\mu \subset \mathcal{D}\}$; Ξ_μ consists of $\mathcal{M}$ parameter sample points μ. We assume this sample subset is representative of the entire set $\mathcal{U}$ in the sense that $\sup_{x\in\mathcal{U}} \inf_{y\in X_\mathcal{M}} \|x-y\|_X$ is much smaller than the approximation we envision through the interpolation process. Here $X_\mathcal{M}$ is the vectorial space spanned by W^u. We assume that the dimension of $X_\mathcal{M}$ is $\mathcal{M}$.*

We will now subject the empirical interpolation procedure described above to some tests: the abstract formulation of the problems we are going to solve can be stated as follows: given a space $\mathcal{U} \subset X \subset L^\infty(\Omega)$, we will construct a space $X_M \subset X$ and an interpolant $\mathcal{I}_M \in X_M$ such that for a given function $u \in \mathcal{U}$, $\|u - \mathcal{I}_M[u]\|_{L^\infty(\Omega)} \to 0$ rapidly as $M \to \infty$. We can classify the problems into two distinct categories:

1. $\mathcal{U} \equiv X \equiv C^m$ and X_M spans the same space as a preselected universal approximation space; here we are interested in constructing a well-conditioned set of basis functions in X_M and the corresponding magic points;

2. $\mathcal{U}$ is a set of functions on the parametric manifold, X_M is a — a priori not known — finite dimensional space in X is some well-defined function spaces such as Sobolev spaces.

3 Polynomial Interpolation

We consider the first category of problems. In particular, X_M consists of polynomial functions. The purpose of this section is to (i) test the empirical interpolation process in well-documented situations in order to first measure where magic points stand with respect to some optimal results, and (ii) understand if the order at which the basis functions are processed affects the Lebesgue constant.

3.1 One dimension

We consider a domain $\Omega_{1\mathrm{d}} \equiv [-1, 1]$ and construct $X_M(\Omega_{1\mathrm{d}})$ and the associated magic points based on:

(a) monomials, $W_n^P(\Omega_{1\mathrm{d}}) = \{x^i, x \in \Omega_{1\mathrm{d}}, 0 \leq i \leq n\}$, $0 \leq n \leq n_{\max}$; and

(b) Legendre polynomials, $W_n^L(\Omega_{1\mathrm{d}}) = \{L_i(x), x \in \Omega_{1\mathrm{d}}, 0 \leq i \leq n\}$, $0 \leq n \leq n_{\max}$ where L_i is the Legendre polynomial of order i.

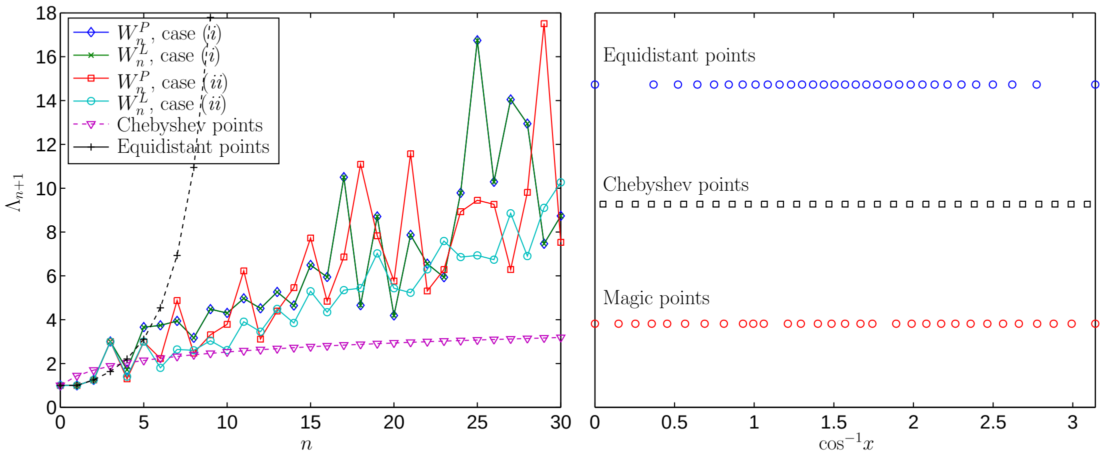

Figure 1: (a) Comparison of the Lebesgue constant, $\Lambda_{M=n+1}$ for magic points obtained through different constructions (case (i) refers to increasing polynomial order and case (ii), greedy algorithms) with that obtained for Chebyshev points and the uniform grid. (b) $\cos^{-1}$ of the distribution of magic points compared to Chebyshev points and the uniform grid, for $\Omega_{1\mathrm{d}}$.

Note that $X_M = \mathrm{span}\ \{W_n^P(\Omega_{1\mathrm{d}})\} = \mathrm{span}\ \{W_n^L(\Omega_{1\mathrm{d}})\}$ with $M = n+1$. To examine the effects of ordering on the resulting approximation, we apply the empirical interpolation procedure based on two variations: (i) the basis functions are processed in increasing polynomial order; and (ii) the order by which the basis functions are processed is determined by the greedy algorithm. We discretize the space into 2000 intervals and solve the system up to $n_{\max} = 30$. As expected and shown in Figure 1, the choice of the initial approximation spaces does not affect the magnitude of the Lebesgue constant when the basis functions are processed in increasing polynomial orders. Greedy algorithm can result in slightly better Lebesgue constant for some n, although the result is not uniform. In both cases, the Lebesgue constant obtained through our empirical interpolation procedure is close to the (nearly) optimal values obtained based on the Chebyshev points, as shown in Figure 1. Lastly, Figure 1 also shows that the distribution of the empirical interpolation points bears significant resemblance to the Chebyshev points. For comparison, we have also plotted the behavior for equidistant interpolation points. Finally, it should be noted that the Lebesgue constant for the magic point construction is not monotonic as a function of the number of points.

3.2 Triangle

We consider a triangle $\overline{\Omega}_{\mathrm{tri}} \equiv \{(x, y) : x \geq -1, y \geq -1, x + y \leq 0\}$. We define the initial sample set as $W_n^P(\Omega_{\mathrm{tri}}) \equiv \{x^i y^j, (x, y) \in \Omega_{\mathrm{tri}}, i + j \leq n\}$, $0 \leq n \leq n_{\max}$. Then $X_M(\Omega_{\mathrm{tri}}) = \mathrm{span}\ \{W_n^P(\Omega_{\mathrm{tri}})\}$ and $M = \frac{1}{2}(n + 1)(n + 2)$. Since the greedy algorithm leads to smaller Lebesgue constants in most cases, we will apply the greedy algorithm to $W_n^P(\Omega_{\mathrm{tri}})$ (and to all subsequent examples) when determining the magic points. We further discretize the domain such that the smallest division in each direction is 0.01. Figure 2 shows the growth of the Lebesgue constant with n up to $n_{\max} = 12$. Compared to the optimal points obtained in [10] and [5], the Lebesgue constants for our empirical interpolation points are not too far off, as shown in Table 1. In addition, these points are obtained through a simple procedure, in the absence of any sophisticated optimization process. Lastly, we observe that the distribution of the empirical interpolation points again bears strong resemblance to those reported in [10], as shown in Figure 2 for $n = 12$.

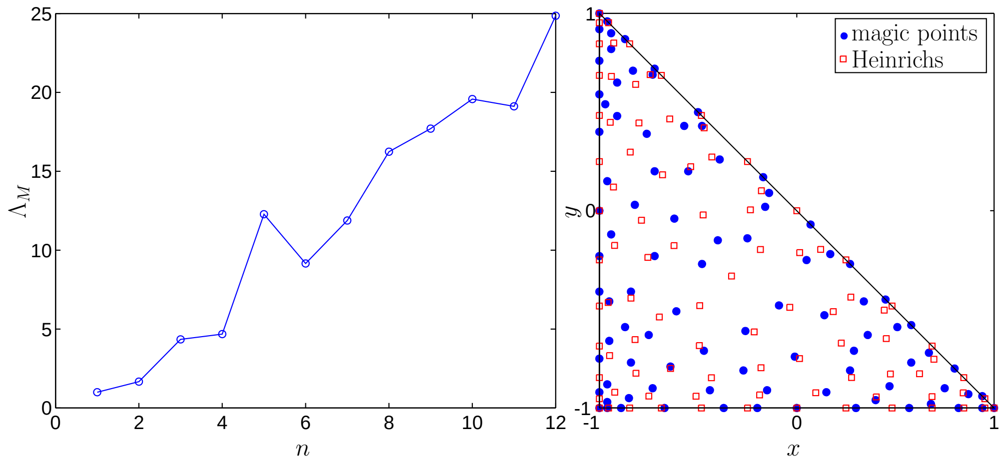

Figure 2: (a) Variation of Lebesgue constant, Λ_M with n where $M = \frac{1}{2}(n+1)(n+2)$, and (b) distribution of magic points compared to [10] for Ω_{tri}.

n	Magic Points	[10]	[5]
6	9.16	3.67	3.79
9	17.70	5.58	5.92
12	24.86	7.12	10.08

Table 1: Comparing the Lebesgue constants for magic points, with that from literature, for Ω_{tri}.

3.3 Hexagon

We define Ω_{hex} as a hexagon inscribed in a circle of radius 1 and an initial sample set given by $W_n^P(\Omega_{\text{hex}}) \equiv \{x^i y^j, (x,y) \in \Omega_{\text{hex}}, i+j \leq n\}$, $0 \leq n \leq n_{\max}$. Then, $X_M(\Omega_{\text{hex}}) = \text{span}\,\{W_n^P(\Omega_{\text{hex}})\}$ with $M = \frac{1}{2}(n+1)(n+2)$. The growth of the Lebesgue constants with n, and the distribution of the magic points (for the case with increasing n) are shown in Figure 3. We have not found any analysis for the best position of the interpolation points over such a simple domain, the good behavior of the Lebesgue constant associated with the magic points is one of the interests of the method.

3.4 Lunar Croissant

We consider now a non-convex domain of "lunar croissant" shape, $\Omega_{\text{cro}} \equiv \Omega^1_{\text{cir}} \backslash \Omega^2_{\text{cir}}$, where Ω^1_{cir} and Ω^2_{cir} are two unit circles centered at $(0,-0.5)$ and $(0,0.5)$, respectively. We define an initial sample set as $W_n^P(\Omega_{\text{cro}}) \equiv \{x^i y^j, (x,y) \in \Omega_{\text{cro}}, i+j \leq n\}$, $0 \leq n \leq n_{\max}$, and $X_M(\Omega_{\text{tri}}) = \text{span}\,\{W_n^P(\Omega_{\text{tri}})\}$ with $M = (n+1)^2$. We show in Figure 4 the Lebesgue constant Λ_n as a function of n and the distribution of the magic points for $n = 12$. We observe that the growth of the Lebesgue constant with n is quite similar to those in the triangle and hexagon cases. We know of neither exact nor computed values for the optimal (or even near optimal) point set over the domain Ω_{cro}.

3.5 Tetrahedron

We define Ω_{tet} as a three-dimensional simplex in $\mathbb{R}^3$ with vertices at $(0,0,0)$, $(0,0,1)$, $(0,1,0)$ and $(1,0,0)$ and an initial sample set given by $W_n^P(\Omega_{\text{tet}}) \equiv \{x^i y^j z^k, (x,y,z) \in \Omega_{\text{tet}}, i+j+k \leq n\}$, $0 \leq n \leq n_{\max}$. Then, $X_M(\Omega_{\text{tet}}) = \text{span}\,\{W_n^P(\Omega_{\text{tet}})\}$ with $M = \frac{1}{6}(n+1)(n+2)(n+3)$. The application of the empirical interpolation procedure yields Lebesgue constants shown in Table 2 for $n \leq n_{\max} = 9$. It is compared to results from [12] and [6] obtained through optimization procedures. Again, in comparison to the best known approximation, the empirical interpolation procedure performs reasonably well.

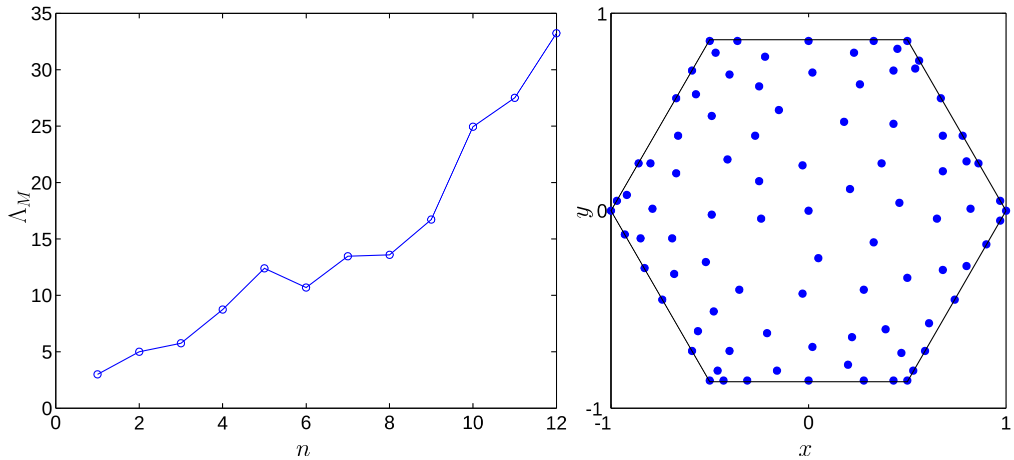

Figure 3: (a) Variation of Lebesgue constant, Λ_M with n where $M = \frac{1}{2}(n+1)(n+2)$, and (b) distribution of magic points, for Ω_{hex}.

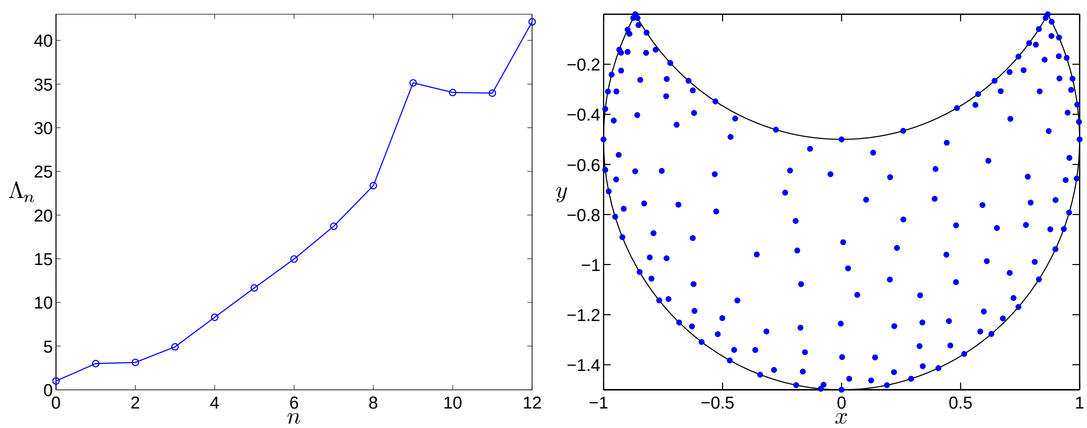

Figure 4: Results for a "lunar croissant" domain Ω_{cro}: (a) variation of the Lebesgue constant Λ_n with n, and (b) distribution of magic points for $n = 12$.

n	Magic Points	[12]	[6]
2	2.0	2.0	2.0
3	3.80	2.93	2.93
4	8.70	4.07	4.11
5	9.77	5.38	5.62
6	15.27	7.53	7.36
7	31.04	10.17	9.37
8	34.31	14.63	12.31
9	62.99	20.46	15.69

Table 2: Comparing the Lebesgue constants for magic points with that from literature, for Ω_{tet}.

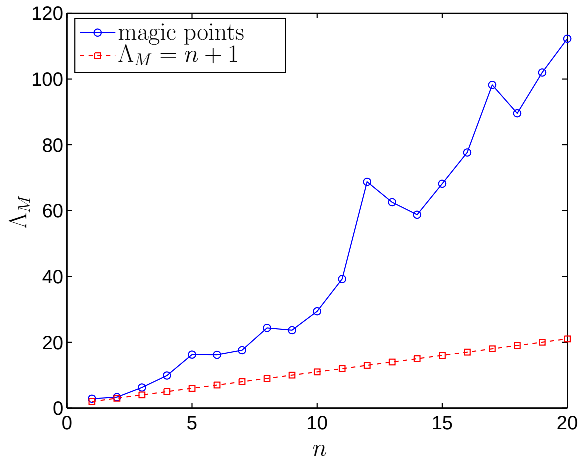

Figure 5: Variation of the Lebesgue constant, Λ_M with n where $M = (n+1)^2$, for Ω_{sph}.

4 Different types of approximations

4.1 Spherical harmonics on the surface of a sphere

We consider the surface of the sphere $\Omega_{\text{sph}} \equiv \{|\mathbf{x}| = 1, \mathbf{x} \in S^2 \subset \mathbb{R}^3\}$ and define an initial sample set given by $W_n^S(\Omega_{\text{sph}}) \equiv \{Y_{lm}(\mathbf{x}), \mathbf{x} \in \Omega_{\text{sph}}, 0 \le l \le n, |m| \le l\}$, $0 \le n \le n_{\max}$, where $\{Y_{lm}(\mathbf{x})\}$ is an orthonormal set of spherical harmonics. Then, $X_M(\Omega_{\text{sph}}) = \text{span}\,\{W_n^S(\Omega_{\text{sph}})\}$ with $M = (n+1)^2$. The application of the empirical interpolation procedure yields Lebesgue constant that grows as shown in Figure 5 for $n \le n_{\max} = 20$; this is compared to the improved rate of $n+1$ obtained in [25] through an optimization procedure. The deviation here is sensibly larger with respect to the best fit, though still acceptable if we compare it to the other earlier results quoted before [25] where a $\mathcal{O}(n^2)$ is documented.

Remark 4. *An important remark is now in order. The magic points in T_M are defined recursively, which is not at all the case for other approaches, in particular the points proposed in [25]. Starting from a maximal space X_{max}, the associated approximation spaces X_M are hierarchical, i.e. $X_1 \subset X_2 \subset \ldots \subset X_M \subset X_{\max}$. In order to illustrate this distinction, we first look at the problem of choosing $M/2$ points from the M points proposed by Sloan [25] for a given n that gives the minimum Lebesgue constant when approximating using the first $M/2$ basis functions in W_n^S. Clearly, as the number of possible combinations increases exponentially fast as n increases. Considerable effort is required to find a good combination. On the contrary, with empirical interpolation procedure, determining a good combination of $M/2$ points out of the M number of magic points is simple — we simply choose the first $M/2$ points.*
To demonstrate how good these magic points are, we randomly choose 1000 combinations of $M/2$ points from the M Sloan points and search through these sets of points for the minimum Lebesgue constant. We compare the resulting Lebesgue constants with that obtained using the first $M/2$ magic points. For $n = 4$, Sloan points gives 6.44 vs 4.93 for magic points. For $n = 10$, Sloan points gives 138.56 vs 20.25 for magic points. Here the Lebesgue constants for the magic points are obtained without using the greedy algorithm, i.e. the basis functions are processed in the order given in W_n^S.

Remark 5. *Another remark is the versatility of this approach with respect to the domain. We have considered the domain on the sphere delimited by reducing the angle to $[\pi/3, 5\pi/6] \times [2\pi/3, 4\pi/3]$, so it is more or less a curve surface. Over a very fine grid of 600×600 the best Lebesgue constant that we could get for $n = 10$ is 36 as shown in figure 6. There is also signficicant resemblance between the magic points and the tensorized Chebyshev points, as shown in Figure 6. Here again no reference could be found for interpolating with spherical harmonics over a portion of a sphere.*

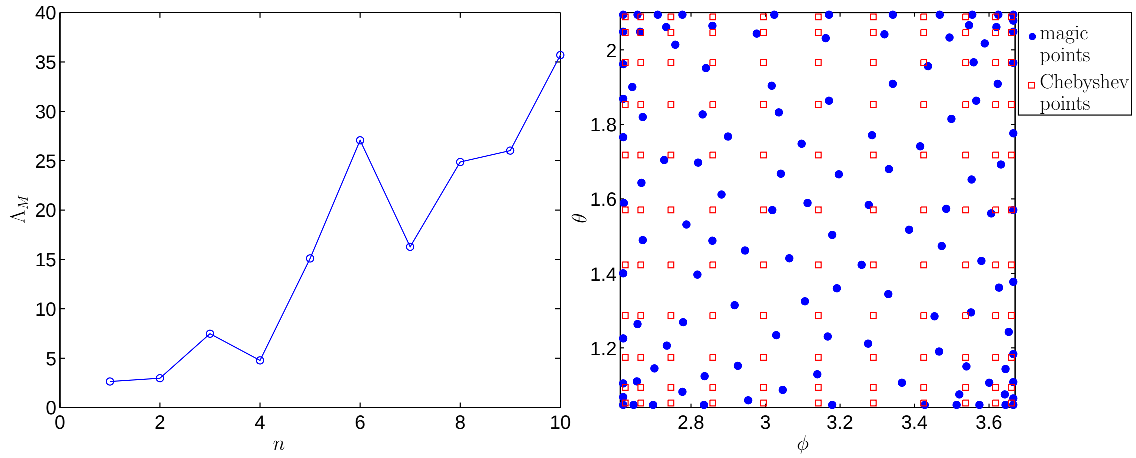

Figure 6: (a) Variation of the Lebesgue constant, Λ_M with n where $M = (n+1)^2$, and (b) distribution of magic points, compared to Chebyshev points, for part of $\Omega_{\rm sph}$ given by $[\pi/3, 5\pi/6] \times [2\pi/3, 4\pi/3]$.

4.2 Parameter-dependent functions

We now examine the second category of problems outlined in Section 2. Here, we are interested in approximating parameter-dependent transcendental functions $f(x, \mu)$. In particular, we have in mind functions that are complicated to evaluate but have a smooth dependency on some parameters such as $e^{g(x,\mu)}$, convoluted functions, smooth empirical data varying smoothly in time or space etc. To illustrate the potential computational savings resulting from the use of empirical interpolation procedure, we examine the following convoluted function

$$f(\mathbf{x}, \mu) = \int_\Omega l(\mathbf{x}', \mu) g(\mathbf{x}, \mathbf{x}') d\mathbf{x}'. \tag{14}$$

For every new μ, a full evaluation of f will require, for each $\mathbf{x}$ point the computation of an integral (in $\mathbf{x}'$) which may be done by numerical integration based on a large enough set of points (say $\mathcal{N}$ points) Assume, for the sake of simplicity, that we want to compute f at any of these $\mathcal{N}$ points, this will required $\mathcal{O}(\mathcal{N}^2)$ operations. However, if for a given Ξ_μ, we construct an approximation space of dimension M and the associated magic points for $f(\,\cdot\,, \mu)$, we will only required $2(M\mathcal{N}) + M^2$ operations — we only evaluate the integral at M magic points (which gives $M\mathcal{N}$ operations), solve for the coefficients by inverting a $M \times M$ triangular matrix, then require another $M\mathcal{N}$ to get an approximation of f at every $\mathcal{N}$ points .

As an example, we consider a domain $\Omega_{\rm rec} = [-0.5, 0.5] \times [-0.5, 0.5]$, $\mu \in [1, 10]$, $\mathbf{x} \equiv (x, y)$, $l(\mathbf{x}, \mu) = \sin(2\pi\mu|\mathbf{x}|)$, and $g(\mathbf{x}) = \frac{50}{\pi} \exp(-50|\mathbf{x}|^2)$. We construct our approximation based on the sample set $W^f(\Omega_{\rm rec}) = \{f(\,\cdot\,, \mu), \mu \in \Xi_\mu \subset [1, 10]\}$. Table 3 shows that the error $\|f(\,\cdot\,, \mu) - \mathcal{I}_M[f(\,\cdot\,, \mu)]\|_{L^\infty(\Omega_{\rm rec})}$ decreases exponentially and the Lebesgue constants are generally small for all M. Thus, the approximation leads to fast evaluation of f with minimal loss of accuracy. This may have applications in areas such as animation where μ represent temporal variables, the regeneration of 3D tomographic data sets where μ represent spatial variables, or the reduced basis methods, as will be illustrated in the section.

M	$\Vert f(\,\cdot\,,\mu) - \mathcal{I}_M[f(\,\cdot\,,\mu)]\Vert_{L^\infty(\Omega_{\text{rec}})}$	Λ_M
2	8.60 E − 1	1.51
3	4.19 E − 1	1.69
4	2.74 E − 1	1.98
5	1.24 E − 1	2.43
6	9.80 E − 2	3.16
7	6.59 E − 2	5.14
8	6.00 E − 2	3.89
9	9.10 E − 3	2.48
10	3.88 E − 3	3.28
11	1.74 E − 3	4.38
12	6.44 E − 4	4.56
13	2.82 E − 4	4.24
14	6.35 E − 5	5.94
15	6.09 E − 6	5.23

Table 3: Actual error between $f(\cdot,\mu)$ of Section 4.2 and its iterpolation together with the associated Lebesgue constant.

5 Two applications for the approximation of the solutions to some PDEs

5.1 Reduced basis method

This is the frame actually for which the magic points have been constructed... We consider a weak formulation of μ-parametrized nonlinear elliptic PDEs of the form

$$\mu a_0(u(\mu),v) + \int_\Omega g(u(\mu))v = f(v), \quad \forall v \in H_0^1(\Omega). \tag{15}$$

A particular instantiation considered here is as follows

$$a_0(w,v) = \int_\Omega \nabla w \cdot \nabla v, \qquad f(v) = \int_\Omega v, \qquad g(w) = |w|^{2/3}w, \tag{16}$$

where $\Omega =]0,1[\in \mathbb{R}$, w and $v \in H_0^1(\Omega)$, and $\mu \in \mathcal{D} \equiv [0.01, 1]$; note the solution $u(\mu)$ develops a boundary layer at $x = 0$ and $x = 1$ for μ close to 0.01.

We now introduce the nested samples, $S_N^u = \{\mu_1^u \in \mathcal{D}, \ldots, \mu_N^u \in \mathcal{D}\}$, $1 \le N \le N_{\max}$, and associated nested Lagrangian [21] reduced-basis spaces $W_N^u = \text{span}\{u(\mu_n^u),\ 1 \le n \le N\} = \text{span}\ \{\zeta_n,\ 1 \le n \le N\}$, $1 \le N \le N_{\max}$, where $u(\mu_n^u)$ is the solution of (15) at $\mu = \mu_n^u$ and $\zeta_n, 1 \le n \le N$ are the orthonormalized bases of $u(\mu_n^u)$, $1 \le n \le N$ with respect to $(\cdot,\cdot)_X$ (obtained through a Gram-Schmidt process). The classical reduced-basis approximation [13, 15, 22, 24, 8] is then obtained by a standard Galerkin projection: given $\mu \in \mathcal{D}$, $u_N(\mu) \in W_N^u$ satisfies

$$\mu a_0(u_N(\mu),v) + \int_\Omega g(u_N(\mu))\ v = f(v), \quad \forall v \in W_N^u. \tag{17}$$

Unfortunately, the presence of *strong* nonlinearity in g does not allow an efficient *offline-online* procedure outlined in [23, 18]. As a result, although the dimension of the system (17) is small, solving it is actually expensive [4, 7].

To obtain an *inexpensive* reduced-oder model of the nonlinear problem (15), we apply the empirical interpolation procedure on $\{g(u(\mu)), \mu \in \Xi_\mu\}$ of size $\mathcal{M} = 51$ to develop a collateral reduced-basis expansion

$g_M^{u_{N,M}}(x;\mu)$ for the nonlinear term $g(u_N(\mu))$ as

$$g_M^{u_{N,M}}(x;\mu) = \sum_{m=1}^{M} \varphi_{M\,m}(\mu) q_m(x) \ , \tag{18}$$

We next replace $g(u_N(\mu))$ — as required in our reduced-basis projection for $u_N(\mu)$ — with $g_M^{u_{N,M}}(x;\mu)$. Our reduced-basis approximation is thus: given $\mu \in \mathcal{D}$, $u_{N,M}(\mu) \in W_N^u$ satisfies

$$\mu a_0(u_{N,M}(\mu), v) + \int_\Omega g_M^{u_{N,M}}(x;\mu) v = f(v), \quad \forall\, v \in W_N^u \ . \tag{19}$$

Inserting $u_{N,M}(\mu) = \sum_{j=1}^N u_{N,M\,j}(\mu)\zeta_j$ and (18) into (19) yields

$$\mu \sum_{j=1}^{N} A_{i\,j}^N u_{N,M\,j}(\mu) + \sum_{m=1}^{M} C_{i\,m}^{N,M} \varphi_{M\,m}(\mu) = F_{N\,i}, \quad 1 \le i \le N \ ; \tag{20}$$

where $A^N \in \mathbb{R}^{N\times N}, C^{N,M} \in \mathbb{R}^{N\times M}, F_N \in \mathbb{R}^N$ are given by $A_{i\,j}^N = a_0(\zeta_j,\zeta_i), 1 \le i,j \le N$, $C_{i\,m}^{N,M} = \int_\Omega q_m\zeta_i, 1 \le i \le N, 1 \le m \le M$, and $F_{N\,i} = f(\zeta_i), 1 \le i \le N$, respectively.

Furthermore, we note that $\varphi_M(\mu) \in \mathbb{R}^M$ is given by

$$\sum_{k=1}^{M} B_{m\,k}^M \varphi_{M\,k}(\mu) = g(u_{N,M}(x_i,\mu)) = g\Big(\sum_{n=1}^{N} u_{N,M\,n}(\mu)\zeta_n(x_m)\Big), \quad 1 \le m \le M \ . \tag{21}$$

We then substitute $\varphi_M(\mu)$ from (21) into (20) and let $D^{N,M} = C^{N,M}(B^M)^{-1}$ to obtain the following nonlinear algebraic system

$$\mu \sum_{j=1}^{N} A_{i\,j}^N u_{N,M\,j}(\mu) + \sum_{m=1}^{M} D_{i\,m}^{N,M} g\Big(\sum_{n=1}^{N} \zeta_n(x_m) u_{N,M\,n}(\mu)\Big) = F_{N\,i}, \quad 1 \le i \le N \ , \tag{22}$$

which can be solved efficiently by using a Newton method [4, 7] to yield $u_{N,M\,j}(\mu), 1 \le j \le N$, for any parameter value μ in $\mathcal{D}$.

In a similar manner, to get a comparison of this approach with a more classical one, we also develop a reduced-order model based on a coefficient-function approximation of the nonlinear term $g(u_N(\mu))$ using polynomials $x^m, 0 \le m \le M-1$, and associated Chebyshev points $x_m^{\rm che} = (\cos((2m+1)\pi/(2M+2))+1)/2, 0 \le m \le M-1$. We denote by $u_{N,M}^{\rm che}(\mu)$ the reduced-basis approximation using the polynomial approach with Chebyshev points.

We now present numerical results obtained for this particular example. For this purpose, we introduce a parameter sample $\Xi_t \subset \mathcal{D}$ of size 100; we then define $\epsilon_M^g = \max_{\mu\in\Xi_t} \|g(u(\mu)) - g_M^u(x;\mu)\|_{L^\infty(\Omega)}$, $\epsilon_M^{g,\rm che} = \max_{\mu\in\Xi_t} \|g(u(\mu)) - g_M^{u,\rm che}(x;\mu)\|_{L^\infty(\Omega)}$, $\epsilon_{N,M}^u = \max_{\mu\in\Xi_t} \|u(\mu) - u_{N,M}(\mu)\|_{L^\infty(\Omega)}$, $\epsilon_{N,M}^{u,\rm che} = \max_{\mu\in\Xi_t} \|u(\mu) - u_{N,M}^{\rm che}(\mu)\|_{L^\infty(\Omega)}$; here $g_M^u(x;\mu)$ and $g_M^{u,\rm che}(x;\mu)$ are the approximations of $g(u(\mu))$ obtained using the magic points approach and polynomial approach, respectively. We present in Table 4 ϵ_M^g and $\epsilon_M^{g,\rm che}$ for different values of M. We see that ϵ_M^g converges exponentially with M and significantly faster than $\epsilon_M^{g,\rm che}$. We also tabulate in Table 5 $\epsilon_{N,M}^u$ and $\epsilon_{N,M}^{u,\rm che}$ as a function of N for $M = 8$. Not surprising, we observe the same convergence behavior in terms of the reduced-basis dimension N: while the reduced-basis error $\epsilon_{N,M}^u$ decays exponentially fast with N, the error $\epsilon_{N,M}^{u,\rm che}$ decreases with N for $N \le 5$ and then maintains a fixed value of 3.80 E−03 for $N > 5$ due to poor approximation of the nonlinearity as observed in Table 4.

5.2 One-dimensional quantum harmonic oscillator

We now look at another example of a model reduction method, the modal expansion technique [2]. For linear partial differential equations, the projection onto the eigenmodes of the operator leads to a set of

M	ϵ^g_M	$\epsilon^{g,\text{che}}_M$
1	2.43 E−01	9.94 E−01
2	1.62 E−02	7.35 E−01
3	1.86 E−03	1.73 E−01
4	1.28 E−04	1.63 E−01
5	4.21 E−06	1.10 E−01
6	2.18 E−07	8.84 E−02
7	1.15 E−08	6.75 E−02
8	9.22 E−10	4.57 E−02

Table 4: Results for the approximation of $g(u(\mu))$: ϵ^g_M and $\epsilon^{g,\text{che}}_M$ as a function of M.

N	M	$\epsilon^u_{N,M}$	$\epsilon^{u,\text{che}}_{N,M}$
1	8	2.82 E−01	2.82 E−01
2	8	1.50 E−02	1.50 E−02
3	8	5.55 E−04	8.84 E−03
4	8	4.78 E−05	3.96 E−03
5	8	5.71 E−07	3.92 E−03
6	8	4.59 E−08	3.80 E−03
7	8	1.23 E−09	3.80 E−03
8	8	1.93 E−10	3.80 E−03

Table 5: Results for the reduced-basis approximation: $\epsilon^u_{N,M}$ and $\epsilon^{u,\text{che}}_{N,M}$ as a function of N for $M = 8$.

decoupled differential equations. This is particularly advantageous in dynamic response analysis due to order of reductions in problem size. However, the initial projection of the initial condition onto the eigenspace is usually required, leading to an operation count which depends on $\mathcal{N}$, the discretization of the underlying computational domain. We will demonstrate how empirical interpolation technique provides a inexpensive surrogate to this projection step. As an example, we consider a time-dependent Schrödinger equation for a harmonic oscillator:

$$\mathbf{i}\frac{\partial}{\partial t}\psi(x,t) = -\frac{1}{2}\frac{\partial^2}{\partial x^2}\psi(x,t) + \frac{1}{2}\omega_0^2 x^2 \psi(x,t), \tag{23}$$

where $x \in \Omega_{\text{1d,SHO}} \equiv [-15, 15]$. Given an initial solution $\psi(x,0)$, the solution can be approximated by

$$\psi(x,t) = \sum_{i=0}^{n} c_i \phi_i(x) e^{-\mathbf{i}E_i t}, \tag{24}$$

where $n+1$ is the number of basis functions considered; $\phi_i(x)$ and E_i are solution to the following static harmonic oscillator equation

$$E_i \phi_i(x) = -\frac{1}{2}\frac{\partial^2}{\partial x^2}\phi_i(x) + \frac{1}{2}\omega_0^2 x^2 \phi_i(x); \tag{25}$$

and c_i is given by

$$c_i = \int_{-\infty}^{\infty} \phi_i^*(x)\psi(x,0)dx. \tag{26}$$

Note that the analytical solutions to $\phi_i(x)$ and E_i exist but evaluation of c_i based on (26) can be tedious and expensive, especially if the problem is multidimensional. For example, evaluation of c_i for all $i = 0, \ldots, n$ based on the Newton-Cotes Formulae using $\mathcal{N}$ nodes would require $O((n+1)\mathcal{N})$ operations. Our goal is to approximate c_i based on the empirical interpolation procedure. Therefore, given $W_n^\phi = \{\phi_i(x), x \in$

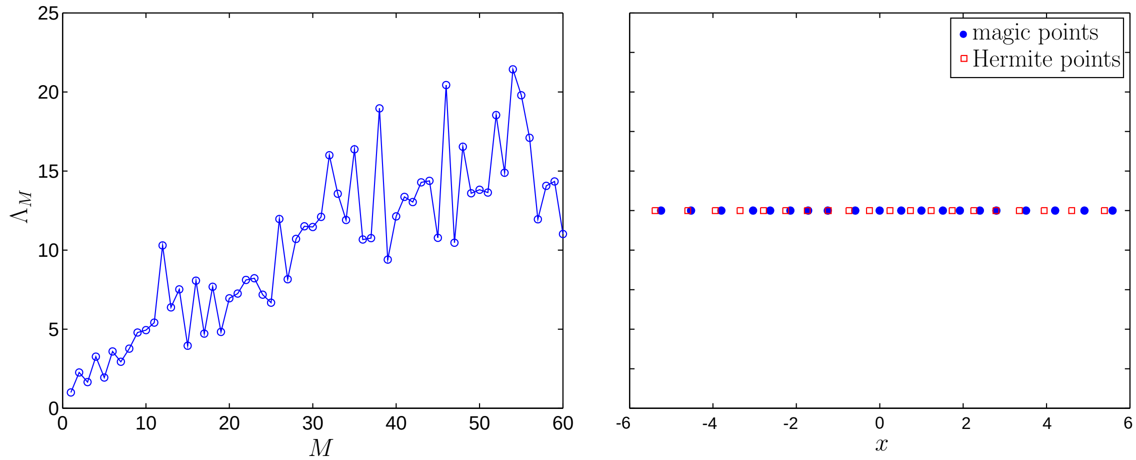

Figure 7: (a) Variation of Lebesgue constant, Λ_M with M, and (b) distribution of the magic points compared to the zeros of the Hermite polynomials for $\omega_o = 1$, for the quantum harmonic oscillator problem for $M = 20$.

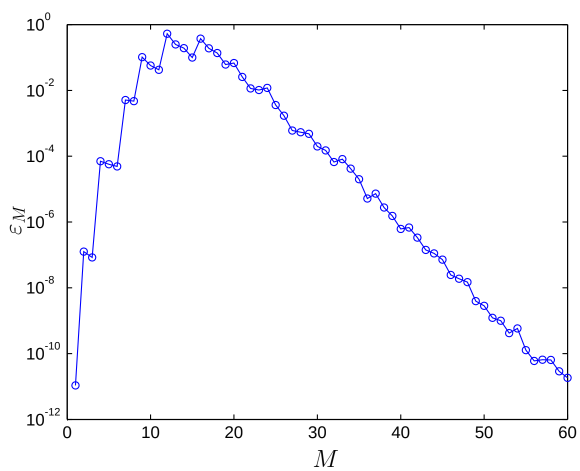

Figure 8: Variation of ε_M with M.

$\Omega_{1\mathrm{d,SHO}}, 0 \le i \le n\}$, we can construct X_M and the associated set of magic points $T_M = \{x_i, 0 \le i \le n\}$ and the interpolation matrix B based on the empirical interpolation procedure. Here, $M = n+1$. Then we approximate c_i by $\tilde{c}_i$, where $\sum_{j=0}^{n} B_{ij}\tilde{c}_j = \psi(x_i, 0)$, $0 \le i \le n$. The operations count is only $O((n+1)^2)$. We achieve an operation count that is independent of $\mathcal{N}$. The growth of the Lebesgue constant Λ_M with M is shown in Figure 7 — they are in general small.

We now consider a particular example where $\psi(x,0) = \left(\frac{\omega}{\pi}\right)^{1/4} e^{\frac{1}{2}\omega(x-x_0)^2}$ (with $\omega = 2$). For this initial condition, analytical solution, $\psi_a(x,t)$ is available [9]. We first define $\Xi_x \in [-15, 15]$ of size 1000 and $\Xi_t \in [0, 5]$ of size 1000. We then define $\varepsilon_M = \max_{t\in\Xi_t} \max_{x\in\Xi_x} |\psi_a(x,t) - \psi(x,t)|$. Figure 8 shows that the error ε_M decreases very rapidly with M. (The initial increase in the error is simply because $\phi_0(x)$ is close to $\psi(x,0)$, of course it would not be the case if a pure Galerkin method based on X_M was used??).

6 An *a posteriori* analysis

In this section, we propose an *a posteriori* error estimator for our approximation. In [7], it was proven that if the function we are approximating, say φ, is in X_{M+1}, then $\varepsilon_M \equiv \|\varphi - \mathcal{I}_M[\varphi]\|_{L^\infty(\Omega)} = \hat{\varepsilon}_M$ where

n	M	$\lvert\varphi_{1d}(x_{M+1}) - \mathcal{I}_M[\varphi_{1d}(x_{M+1})]\rvert$	$\lVert\varphi_{1d} - \mathcal{I}_M\varphi_{1d}\rVert_{L^\infty}$	η_M
2	3	7.27 E−2	7.79 E−2	1.07
4	5	7.47 E−3	7.52 E−3	1.01
6	7	6.18 E−4	6.70 E−4	1.08
8	9	3.84 E−5	3.84 E−5	1.00
10	11	1.69 E−6	1.72 E−6	1.02
12	13	3.08 E−8	4.02 E−8	1.30
14	15	1.65 E−9	1.65 E−9	1.00
16	17	6.33 E−11	6.73 E−11	1.06
18	19	1.39 E−12	1.39 E−12	1.00
20	21	2.50 E−14	2.51 E−14	1.00

Table 6: Comparison between the error estimate and the actual error, for φ_{1d}.

n	M	$\lvert\varphi_{2d}(x_{M+1}) - \mathcal{I}_M[\varphi_{2d}(x_{M+1})]\rvert$	$\lVert\varphi_{2d} - \mathcal{I}_M\varphi_{2d}\rVert_{L^\infty}$	η_M
2	9	1.13 E−1	6.32 E−1	5.59
4	25	1.43 E−1	1.66 E−1	1.16
6	49	2.03 E−2	2.24 E−2	1.10
8	81	7.23 E−4	1.46 E−3	2.02
10	121	5.36 E−5	1.06 E−4	1.98
12	169	2.76 E−6	2.78 E−6	1.01
14	225	1.04 E−8	1.31 E−7	12.60
16	289	2.67 E−9	4.88 E−9	1.83
18	361	4.98 E−11	1.16 E−10	2.33
20	441	2.57 E−12	2.78 E−12	1.08

Table 7: Comparison between the error estimate and the actual error, for φ_{2d}.

$\hat{\varepsilon}_M = |\varphi(x_{M+1}) - \mathcal{I}_M[\varphi(x_{M+1})]|$. However, in general $\varphi \notin X_{M+1}$ and hence $\|\varphi - \mathcal{I}_M[\varphi]\|_{L^\infty(\Omega)} \geq \hat{\varepsilon}_M$, and $\hat{\varepsilon}_M$ is thus a lower bound. However, if $\|\varphi - \mathcal{I}_M\varphi\|_{L^\infty(\Omega)} \to 0$ very fast, we expect the effectivity, $\eta_M = \varepsilon_M/\hat{\varepsilon}_M$ to be good. In addition, determination of x_{M+1} is very inexpensive — we only need to do an additional iteration of the empirical interpolation procedure.

As an example, we choose to approximate through polynomial interpolation on magic points a gaussian function, $\varphi_{1d}(x) = e^{-x^2}$ in one dimension (on a segment), and $\varphi_{2d}(x,y) = e^{-(x^2+y^2)}$ in two dimensions (over a triangle). Table 6 and 7 show that results are good — η_M is in general very small. In the one dimensional case, a good estimator is obtained for $\mathcal{I}_M$ at all $M \leq M_{\max}$. However, in the two dimensional case, a good estimator is only obtained for $\mathcal{I}_M$ when $M = \frac{1}{2}(n+1)(n+2)$. This is because the polynomial approximation of the gaussian function is good only if all monomials of order $\leq n$ is included. Thus, good effectivity is always obtained for the one dimensional case, and $\frac{1}{2}(n+1)(n+2)$ for the two dimensional case. For a non-regular function, we obtain similar results: in Table 8, we show the error estimate and the actual error resulting from a polynomial approximation of $\varphi_{\text{irr}} = |x^3y^3|$ on the triangle. Again, the effectivities is good when the complete set of monomials of degree $\leq n$ is included, but due to discontinuity in higher derivative, we have a much lower convergence rate.

7 Conclusions

We have presented a general multipurpose interpolation method for selecting interpolation points which we dub "magic points". For the problems in which the interpolating functions are *not* given, our method also provides the construction of such functions. The proposed method is very simple to implement and extremely efficient, since unlike many other methods it does not require optimization procedures. We illustrate many of

n	M	$\lvert\varphi_{\rm irr}(x_{M+1}) - \mathcal{I}_M[\varphi_{\rm irr}(x_{M+1})]\rvert$	$\lVert\varphi_{\rm irr} - \mathcal{I}_M\varphi_{\rm irr}\rVert_{L^\infty}$	η_M
2	9	7.95 E−2	1.59 E−1	2.00
4	25	3.88 E−2	1.47 E−1	3.79
6	49	2.44 E−3	1.95 E−2	8.00
8	81	4.26 E−3	2.42 E−2	5.68
10	121	1.37 E−3	3.74 E−3	2.73
12	169	3.75 E−3	5.66 E−3	1.51
14	225	2.96 E−4	5.69 E−4	1.92
16	289	5.01 E−5	5.80 E−4	11.58
18	361	1.29 E−4	3.00 E−4	2.33
20	441	3.09 E−4	5.72 E−4	1.85

Table 8: Comparison between the error estimate and the actual error, for $\varphi_{\rm irr}$.

its attractive features through several numerical examples in polynomial interpolation, parameter-dependent functions, and the approximation of solutions of parametrized PDEs. In the case of polynomal interpolation, results show that the distribution of magic points is quite similar to that of optimal interpolation points and that the Lebesgue constant is close to the optimal values reported in the open literature. We further demonstrate the versality of the method with non-standard domains whereby we are not aware of any optimal (or even near optimal) point settings. In approximating parameter-dependent functions, the method is superior to classical polynomial interpolation methods (e.g., Chebyshev points with polynomial approximation) thanks to its good choice of both interpolating function and point sets that are adaptive to the parameter dependence. In approximating the solution of parametrized PDE, the method helps to establish an efficient reduced order model by constructing a coefficient-function approximation of the nonlinear terms, which results in significant computational savings relative to standard discretization methods.

Lastly, we wish to emphasize that the method can be applicable and may prove advantageous in a variety of applications involving image and pattern recognition, data compression, field reconstruction, fast rendering and visualization in animation, numerical integration of smooth functions on irregular domains. (See [17, 16] for application of a similar method to face recoginition and optimal sensor placement for field reconstruction.) The good performance and the simplicity of the present method warrant further investigations for these applications.

A An example of a bad Lebesgue constant

Let us consider two sequences of interlaced and increasing real numbers $a_0 < b_0 < a_1 < b_1 < \cdots < a_i < b_i < a_{i+1} < \ldots$ and let χ_i be equal to 1 over $]a_i, b_i[$ and 0 elsewhere.

For $i \geq 1$, we denote by φ_i the L^∞ function given by

$$\varphi_i = \chi_0 + \chi_i - \sum_{j=i+1}^{\infty} \chi_j \tag{27}$$

Then it is an easy matter to realize that the empirical interpolation procedure may actually rank the interpolating function as they are (i.e. leave them in the same order) and choose the interpolation points $x_i = \frac{a_i+b_i}{2}$. (Actually, there are multiple choices here for the points that realize the $\arg\max_{x\in\mathbf{R}} |\varphi_i|$; we could avoid by multiplying the φ_i by a suitable slowly decreasing function.)

Then, for any given M, the Lagrangian functions h_i^M are defined by $h_M^M = \varphi_M$ and, for any i, $1 \leq i < M$

$$h_i^M = \varphi_i + \sum_{j=i+1}^{M} h_j^M \tag{28}$$

so that, by induction, $h_i^M(x_0) = 2^{M-i}$, which is the L^∞ norm of h_i^M. The Lebesgue constant, being the sum of these L^∞ norms, then gives $2^M - 1$.

B Proper sampling procedure of the empirical interpolation approach

We adapt to our interpolation greedy construction, the analysis presented in [3] where the best fit approximation is analyzed. Let us denote by r_M the difference between u and its interpolation over the points x_i, $i = 1, \ldots, M$, i.e.

$$r_M(x; u) = u(x) - \sum_{j=1}^{M-1} \alpha_{M,j}(u) \frac{r_j(x)}{r_j(x_j)}. \tag{29}$$

where the coefficients $\alpha_{M,j}(u)$ satisfy

$$\forall i, i = 1, \ldots, M \quad \sum_{j=1}^{M} \alpha_{M,j}(u) q_j(x_i) = u(x_i)$$

taking into account the triangular structure (with only 1 on the diagonal) we get

$$\alpha_{M,i}(u) = u(x_i) - \sum_{j=1}^{i-1} \alpha_{M,j}(u) q_j(x_i)$$

or again (noticing that $\alpha_{M,j}(u)$ is actually independent of M

$$\frac{\alpha_{M,i}(u)}{r_i(x_i)} = \frac{r_i(x_i; u)}{r_i(x_i)}$$

which is, in absolute value, smaller than 1 from the argmax definition of u_i.

It is then an easy matter to realize by induction, that for $\ell < M$

$$r_\ell(x) \equiv r_\ell(x, u_\ell) = u_\ell(x) + \sum_{j=1}^{\ell-1} \gamma_j^\ell(u) u_j(x), \tag{30}$$

with $|\gamma_i^\ell| \leq 2^{\ell-i-1}$. From the hypothesis stated in theorem 2, we derive that there exists v_j in $\mathcal{Z}_{M-1}$ such that $\|u_j(x) - v_j\|_{\mathcal{Y}} \leq ce^{-\alpha M}$ so that, by setting $v_\ell = v_{\mu_\ell} + \sum_{j=1}^{\ell-1} \gamma_j^\ell v_{\mu_j}$ we get

$$\|r_\ell - v_\ell\|_X \leq c 2^{\ell-1} e^{-\alpha M}. \tag{31}$$

Since dim $X_{M-1} = M - 1$, there exists coefficients β_i $1 \leq i \leq M$, with $\|\beta\|_{\ell^\infty} = 1$ such that $\sum_{i=1}^M \beta_i v_i = 0$. Then

$$\| \sum_{i=1}^{M} \beta_i r_i \|_X = \| \sum_{i=1}^{M} \beta_i (r_i - v_i) \|_X \leq \sqrt{M} 2^{M-1} e^{-\alpha M}, \tag{32}$$

and due to the imbedding of $\mathcal{Y}$ into $L^\infty(\Omega)$,

$$\| \sum_{i=1}^{M} \beta_i r_i \|_{L^\infty(\Omega)} \leq c\sqrt{M} 2^{M-1} e^{-\alpha M}. \tag{33}$$

From the definition of the points x_i, and using the fact that $r_j(x_i) = 0$ if $j > i$, we get first that $|\beta_1||r_1(x_1)| \leq c\sqrt{M} 2^{M-1} e^{-\alpha M}$. Then

$$|\beta_2||r_2(x_2)| \leq c\sqrt{M} 2^{M-1} e^{-\alpha M} + |\beta_1||r_1(x_2)|, \tag{34}$$

again from the definition of x_1

$$|\beta_2||r_2(x_2)| \leq c\sqrt{M}2^{M-1}e^{-\alpha M} + |\beta_1||r_1(x_1)| \leq 2c\sqrt{M}2^{M-1}e^{-\alpha M}, \tag{35}$$

and recursively, for any $m \leq M$

$$|\beta_m||r_m(x_m)| \leq 2^{m-1}c\sqrt{M}2^{M-1}e^{-\alpha M}. \tag{36}$$

Since there exists one j such that $\beta_j = 1$, we deduce, for any $m \geq j$

$$|r_m(x_m)| \leq |r_j(x_j)| \leq 2^{j-1}c\sqrt{M}2^{M-1}e^{-\alpha M}, \tag{37}$$

from which we can further deduce that, by the maximization definition of x_m,

$$\|r_m\|_{L^\infty(\Omega)} \leq c\sqrt{M}2^{M+m-2}e^{-\alpha M}. \tag{38}$$

Hence by the maximization definition of μ_m, for any $\mu \in \mathcal{D}$,

$$\|u(\,\cdot\,,\mu) - \mathcal{I}_m[u(\,\cdot\,,\mu)]\|_{L^\infty(\Omega)} \leq \|r_m\|_{L^\infty} \leq c\sqrt{M}2^{M+m-2}e^{-\alpha M}. \tag{39}$$

Besides, it is an easy matter to check that, for any continuous functions φ,

$$\|\varphi - \mathcal{I}_m[\varphi]\|_{L^\infty(\Omega)} \leq \|\varphi - \mathcal{I}_{m-1}[\varphi] - \mathcal{I}_m[\varphi - \mathcal{I}_{m-1}[\varphi]]\|_{L^\infty(\Omega)} \tag{40}$$

since $\mathcal{I}_m[\mathcal{I}_{m-1}\varphi] = \mathcal{I}_{m-1}\varphi$. Then,

$$\|\varphi - \mathcal{I}_m[\varphi]\|_{L^\infty(\Omega)} \leq c\|\varphi - \mathcal{I}_{m-1}[\varphi]\|_{L^\infty(\Omega)} + \|\mathcal{I}_m[\varphi] - \mathcal{I}_{m-1}[\varphi]\|_{L^\infty(\Omega)}. \tag{41}$$

We note now that $\mathcal{I}_m[\varphi] - \mathcal{I}_{m-1}[\varphi]$ is an element of span $\{u(\,\cdot\,,\mu_i), 1 \leq i \leq m\}$ that vanishes at any x_k; $1 \leq k \leq m-1$ so that it is proportional to r_m, from which we deduce it is maximum at x_m. Since $\mathcal{I}_m[\varphi] - \mathcal{I}_{m-1}[\varphi]$ attains its maximum at point x_m for which $\mathcal{I}_m\varphi$ coincides with φ, we then have

$$\|\mathcal{I}_m[\varphi] - \mathcal{I}_{m-1}[\varphi]\|_{L^\infty(\Omega)} = |\varphi(x_m) - \mathcal{I}_{m-1}[\varphi](x_m)| \leq \max_{x\in\Omega} |\varphi(x) - \mathcal{I}_{m-1}[\varphi](x)| \equiv \|\varphi - \mathcal{I}_{m-1}[\varphi]\|_{L^\infty(\Omega)}. \tag{42}$$

This leads to the estimate, $\forall m$, $1 \leq m \leq M$

$$\|\varphi - \mathcal{I}_m[\varphi]\|_{L^\infty(\Omega)} \leq 2\|\varphi - \mathcal{I}_{m-1}[\varphi]\|_{L^\infty(\Omega)}. \tag{43}$$

We finally derive

$$\|u(\,\cdot\,,\mu) - \mathcal{I}_M[u(\,\cdot\,,\mu)]\|_{L^\infty(\Omega)} \leq 2^{M-j}\|r_j\|_{L^\infty(\Omega)} \leq c2^{2M}\sqrt{M}e^{-\alpha M}, \tag{44}$$

and the result is proven thanks to the conditions over α.

Acknowledgement: The authors want to thank Albert Cohen and Ronald A. DeVore for their input in the paper. N.C. Nguyen, A.T. Patera, and G.S.H. Pau acknowledge the support by DARPA and AFOSR under Grant FA9550-05-1-0114 and by the Singapore-MIT Alliance.

References

[1] M. Barrault, N. C. Nguyen, Y. Maday, and A. T. Patera. An “empirical interpolation” method: Application to efficient reduced-basis discretization of partial differential equations. *C. R. Acad. Sci. Paris, Série I.*, 339:667–672, 2004.

[2] K.-J. Bathe. *Finite element procedures.* Prentice Hall, 1996.

[3] A. Buffa, Y. Maday, A. T. Patera, C. Prud'homme, and G. Turinici. In progress. 2006.

[4] E. Cancès, C. LeBris, N. C. Nguyen, Y. Maday, A. T. Patera, and G. S. H. Pau. Feasibility and competitiveness of a reduced basis approach for rapid electronic structure calculations in quantum chemistry. In *Proceedings of the Workshop for High-dimensional Partial Differential Equations in Science and Engineering (Montreal)*, 2005. Submitted.

[5] Q. Chen and I. Babuška. Approximate optimal points for polynomial interpolation of real functions in an interval and in a triangle. *Comput. Methods Appl. Mech. Engrg.*, 128(3-4):405–417, 1995.

[6] Q. Chen and I. Babuška. The optimal symmetrical points for polynomial interpolation of real functions in the tetrahedron. *Comput. Methods Appl. Mech. Engrg.*, 137(1):89–94, 1996.

[7] M. A. Grepl, Y. Maday, N. C. Nguyen, and A. T. Patera. Efficient reduced-basis treatment of nonaffine and nonlinear partial differential equations. *M2AN (Math. Model. Numer. Anal.)*, 2007, In press.

[8] M. A. Grepl, N. C. Nguyen, K. Veroy, A. T. Patera, and G. R. Liu. Certified rapid solution of partial differential equations for real-time parameter estimation and optimization. In *Proceedings of the 2nd Sandia Workshop of PDE-Constrained Optimization: Towards Real-Time and On-Line PDE-Constrained Optimization*, SIAM Computational Science and Engineering Book Series, 2005. To appear.

[9] P. L. Hagelstein, S. D. Senturia, and T. P. Orlando. *Introductory Applied Quantum and Statistical Mechanics*. Wiley-Interscience, 2004.

[10] W. Heinrichs. Improved Lebesgue constants on the triangle. *J. Comput. Phys.*, 207(2):625–638, 2005.

[11] A. Kolmogoroff. ber die beste annäherung von funktionen einer gegebenen funktionenklasse. *Anals of Math.*, 37:107–110, 1963.

[12] H. Luo and C. Pozrikidis. A Lobatto interpolation grid in the tetrahedron. *IMA J. Appl. Math.*, 71(2):298–313, 2006.

[13] L. Machiels, Y. Maday, I. B. Oliveira, A. T. Patera, and D. V. Rovas. Output bounds for reduced-basis approximations of symmetric positive definite eigenvalue problems. *C. R. Acad. Sci. Paris, Série I*, 331(2):153–158, July 2000.

[14] Y. Maday. Reducedbasis method for the rapid and reliable solution of partial differential equations. In *Proceedings of International Conference of Mathematicians*, Madrid. European Mathematical Society Eds., 2006.

[15] Y. Maday, A. T. Patera, and G. Turinici. Global *a priori* convergence theory for reduced-basis approximation of single-parameter symmetric coercive elliptic partial differential equations. *C. R. Acad. Sci. Paris, Série I*, 335(3):289–294, 2002.

[16] N. C. Nguyen, A. T. Patera, and J. Peraire. A "best points" interpolation method for efficient approximation of parametrized functions, International Journal of Numerical Methods in Engineering, 2007, In press

[17] N. C. Nguyen and J. Peraire. An interpolation method for the reconstruction and recognition of face images, Proceedings of the 2nd International Conference on Computer Vision Theory and Applications (VISAPP), Barcelona, Spain, 2007, pp. 91–96

[18] N. C. Nguyen, K. Veroy, and A. T. Patera. Certified real-time solution of parametrized partial differential equations. In S. Yip, editor, *Handbook of Materials Modeling*, pages 1523–1558. Springer, 2005.

[19] A.T. Patera and G. Rozza *Reduced Basis Approximation and A Posteriori Error Estimation for Parametrized Partial Differential Equations* to appear in (tentative rubric) MIT Pappalardo Graduate Monographs in Mechanical Engineering, Copyright MIT, 2006–2007, http://augustine.mit.edu/methodology/methodology_book.htm.

[20] A. Pinkus. *n-Widths in Approximation Theory*. Springer-Verlag, Berlin, 1985.

[21] T. A. Porsching. Estimation of the error in the reduced basis method solution of nonlinear equations. *Mathematics of Computation*, 45(172):487–496, October 1985.

[22] C. Prud'homme, D. Rovas, K. Veroy, Y. Maday, A. T. Patera, and G. Turinici. Reliable real-time solution of parametrized partial differential equations: Reduced-basis output bound methods. *Journal of Fluids Engineering*, 124(1):70–80, March 2002.

[23] K. Veroy, C. Prud'homme, D. V. Rovas, and A. T. Patera. *A posteriori* error bounds for reduced-basis approximation of parametrized noncoercive and nonlinear elliptic partial differential equations (AIAA Paper 2003-3847). In *Proceedings of the 16th AIAA Computational Fluid Dynamics Conference*, June 2003.

[24] K. Veroy, D. Rovas, and A. T. Patera. *A Posteriori* error estimation for reduced-basis approximation of parametrized elliptic coercive partial differential equations: "Convex inverse" bound conditioners. *Control, Optimisation and Calculus of Variations*, 8:1007–1028, June 2002. Special Volume: A tribute to J.-L. Lions.

[25] R. S. Womersley and I. H. Sloan. How good can polynomial interpolation on the sphere be? *Adv. Comput. Math.*, 14(3):195–226, 2001.